ARMY RESEARCH LABORATORY

Detection of Energetic Materials by Laser Photofragmentation/Fragment Detection and Pyrolysis/Laser-Induced Fluorescence

by Rosario C. Sausa, Vaidhianat Swayambunathan, and Gurbax Singh

ARL-TR-2387 February 2001

The findings in this report are not to be construed as an official Department of the Army position unless so designated by other authorized documents.

Citation of manufacturer's or trade names does not constitute an official endorsement or approval of the use thereof.

Destroy this report when it is no longer needed. Do not return it to the originator.

Army Research Laboratory
Aberdeen Proving Ground, MD 21005-5066

ARL-TR-2387 **February 2001**

Detection of Energetic Materials by Laser Photofragmentation/Fragment Detection and Pyrolysis/Laser-Induced Fluorescence

Rosario C. Sausa and Vaidhianat Swayambunathan
Weapons and Materials Research Directorate, ARL

Gurbax Singh
University of Maryland Eastern Shore, Department of Natural Sciences

Abstract

Trace concentrations of energetic materials such as 2,4,6-trinitrotoluene (TNT), pentaerythritol tetranitrate (PETN), and hexahydro-1,3,5-trinitro-s-triazine (RDX) are detected by laser photofragmentation/fragment detection (PF/FD) spectrometry. In this technique, a single laser operating near 227 nm photofragments the parent molecule and facilitates the detection of the characteristic NO fragment by means of its $A^2\Sigma^+ - X^2\ \Pi$ (0,0) transitions near 227 nm. Fragment detection is accomplished by resonance-enhanced multiphoton ionization (REMPI) with miniature electrodes and by laser-induced fluorescence (LIF) with a photodetector. Experiments are also conducted in the visible region using 453.85-nm radiation for photofragmentation and fragment detection. Sand samples contaminated with PETN and RDX are analyzed by a pyrolysis/LIF technique, which involves pyrolysis of the energetic material with subsequent detection of the pyrolysis products NO and NO^2 by LIF and PF/LIF, respectively, near 227 nm. The application of these techniques to the trace analysis of TNT, PETN, and RDX at ambient pressure in room air is demonstrated with limits of detection (S/N = 3) in the range of low parts-per-billion to parts-per-million for a 20-s integration time with 10–120 μJ of laser energy at 226.8 nm and ~ 5 mJ at 453.85 nm. An increase in detection sensitivity is projected with an increase in laser energy and an improved system design. The analytical merits of these techniques are discussed and compared to other laser-based techniques.

Acknowledgments

We thank R. Pesce-Rodriquez and J. Morris of the U.S. Army Research Laboratory (ARL) and E. Cespedes of the U.S. Army Corps of Engineers, Waterway Experiment Station, for providing us with the samples. We also thank J. Simeonsson of the University of Iowa, R. Pesce-Rodriquez, E. Cespedes, and B. Homan of ARL for many helpful discussions. Support from the National Research Council/ARL Senior Research Associateship Program (V. Swayambunathan) and Summer Faculty Program (G. Singh) is gratefully acknowledged.

INTENTIONALLY LEFT BLANK.

Table of Contents

INTENTIONALLY LEFT BLANK.

List of Figures

List of Tables

INTENTIONALLY LEFT BLANK.

1. Introduction

The application of laser-based methods for detecting trace levels of energetic materials has been an active area of research in recent years [1–6]. The trace detection of these materials finds important military and civilian applications in areas such as mine sweeping operations, aviation security, forensic science, and site characterization for cleanup and remediation measures. The detection sensitivities needed range from low parts-per-trillion (ppt) for mine sweeping operations to hundreds of parts-per-million (ppm) for cleanup of contaminated sites. Although several methods, including pyrolysis with subsequent fragment detection spectroscopy, are available for the analysis of these molecules [2], research that is focused on the development of laser-based methods has become increasingly popular because of the high selectivity and sensitivity and their real-time and *in situ* capabilities [1, 3].

A laser-based technique for energetic material detection that has received considerable attention in recent years is laser photofragmenation/fragment detection (PF/FD) spectrometry [1, 3]. In this technique, an ultraviolet laser both photofragments the energetic molecule and facilitates the detection of the characteristic NO photofragment by resonance-enhanced multiphoton ionization (REMPI) or laser-induced fluorescence (LIF). The NO fragment is characteristic of the NO_2 functional group, which is present in these parent molecules and contributes to the selectivity of the analytical method. The energetic material concentration is inferred from the intensity of the NO REMPI or LIF signal.

Hexahydro-1,3,5-trinitro-s-triazine (RDX), 2,4,6-trinitrotoluene (TNT), and pentaerythritol tetranitrate (PETN) are three of the most powerful and most brisant energetic materials. RDX has been detected by time-of-flight mass spectrometry for analytical applications by the 227-nm [7, 8] or 193-nm [9] laser photofragmenation of the vapor with subsequent REMPI detection of NO by means of its $A^2\Sigma^+-X^2\Pi$ (0,0) transitions near 227 nm or its $A^2\Sigma^+-X^2\Pi$ (3,0), $B^2\Pi-X^2\Pi$ (7,0), and $D^2\Sigma^+-X^2\Pi$ (0,1) transitions at 193 nm. TNT has also been detected by the 227-nm laser photofragmentation of the vapor, with subsequent REMPI [7] detection of NO using mass spectrometry or by LIF [10, 11] detection of NO using photometry. Limits of detection range from

ppt to ppm, depending on the energetic material, laser wavelength, laser energy, and sampling conditions.

PETN has not been detected by PF/FD; although RDX and TNT have been detected by PF/FD, this was done under vacuum conditions with ultraviolet lasers and bulky time-of-flight mass spectrometers. PF/FD detection of these materials at atmospheric pressure in room air is a prerequisite if such a technique is to be used in the field. Also, visible lasers could be potentially more useful than ultraviolet lasers for field applications, particularly those applications that require the laser radiation to be transmitted through optical fibers at long distances, such as in the analysis of contaminated underground soil at depths up to 30 m using laser-based, cone penetrometer systems [12]. Although time-of-flight mass spectrometers offer a high degree of selectivity, they are bulky and cannot be incorporated in many small devices (such as hand-held sensors and cone penetrometer heads), as can miniature electrodes.

In this report, we present PF/FD studies on TNT, RDX, and PETN for real-time and *in situ* detection applications. The detection of the energetic materials is accomplished by both PF/REMPI and PF/LIF at atmospheric pressure in room air. A single laser, operating at 227 nm or 454 nm, photofragments the parent molecule and also facilitates the detection of the characteristic NO photofragment by REMPI with miniature electrodes or by LIF with a photodetector. Sand samples doped with PETN and RDX are analyzed by a pyrolysis/LIF technique, in which the pyrolysis products NO and NO_2 are detected by LIF and PF/LIF, respectively, near 227 nm and 454 nm. The analytical utility of these techniques is demonstrated on these energetic compounds and their limits of detection (LODs) are determined.

2. Experimental

A schematic of the experimental apparatus is presented in Figure 1. Briefly, a compact 10-Hz Neodynium-Yttrium-Aluminum-Garnet (Nd-YAG) pumped dye laser (Continuum Surelite III and Lumonics HyperDye 300), with a frequency doubling beta barium borate crystal, provides10–20 mJ

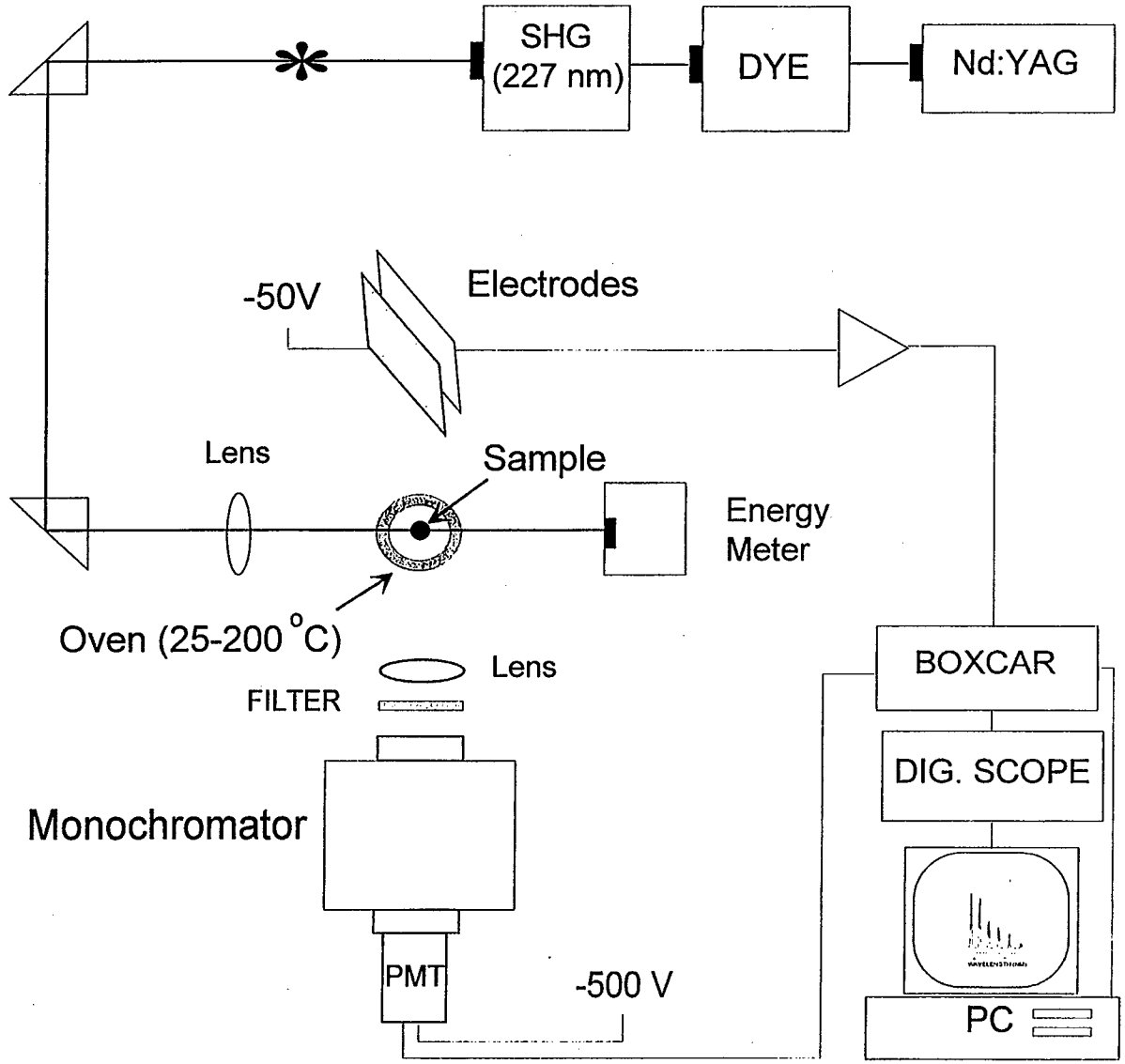

Figure 1. Schematic of the Experimental Apparatus: Second Harmonic Generator (SHG), Computer (PC), Photomultiplier Tube (PMT), and Digital (DIG).

of tunable ultraviolet (UV) radiation in the 225–228-nm wavelength range with a pulse width of ~ 6 ns. The REMPI and LIF experiments were performed at ambient pressure in room air on samples of pure PETN, RDX, and TNT, or on samples of sand doped with known concentrations of the energetic material. The sample cell consists of a miniature, electrically-heated oven, which was designed and built at the U.S. Army Research Laboratory. It housed a removable small glass cup of ~ 5-mm diameter and ~ 10-mm length that contained milligram quantities of the samples. The temperature of the oven was precisely controlled (±1 K) with a thermostat and ranged from room temperature to 473 K. The output vapors, photolysis products, or both were directed to the entrance of a pipe located approximately 20 cm from the top of the oven. The pipe led to an exhaust hood having a linear air velocity of ~ 50 cm/s (Kurtz Air Velocity, Model 441S). The laser beam was steered with quartz prisms and focused with a 25-cm focal-length lens at a distance of 2–3 mm above the tip of the sample tube. At the sampling point, the air-flow velocity was less than <0.05 cm/s, and the LIF and REMPI signal intensities were the same with and without the pipe.

REMPI detection was accomplished with a pair of miniature electrodes (1.25 cm/edge) positioned ~ 2–3 mm above the center of the sample cup. We focused the laser beam at the center of the electrodes to optimize ion collection and minimize the background signal from photoelectron emission. The ion signal from the electrodes was amplified with a current amplifier (Keithley Model 427), which was set at a gain and time constant of 10^6 V/A and 0.01 ms, respectively. The ion signal increased linearly with increasing voltage across the electrodes (0–120 V) for all three compounds. A nominal voltage of 50 V was used for the REMPI spectral recordings and LOD measurements.

For the LIF experiments, the fluorescence was collected with a 8-cm focal-length lens at an angle normal to the laser excitation beam and focused onto the slits of a 0.125- or 0.5-m monochromator (Jarrell Ash or Spex-500) equipped with a photomultiplier tube (Hamamatsu R955). A 250-nm interference filter (FWHM, 30 nm) was also used for signal discrimination for minimizing the intensity of the scattered light. We recorded the excitation spectra by setting the monochromator at 237 nm, corresponding to the NO $A^2\Sigma^+ - X^2\Pi$ (0,1) band, and scanning the laser at a rate of 0.003 or 0.005 nm/s; we recorded the emission spectra by setting the excitation laser near 227 nm and

scanning the monochromator at a rate of 0.1 nm/s. The alignment of the detection optics was optimized using the strong LIF signal from PETN.

We recorded the REMPI and LIF excitation spectra with 10-shot averaging, using a boxcar integrator (Stanford Research Systems, SRS-250) interfaced to a personal computer. A 125-MHz digital oscilloscope (LeCroy, Model 9400) was employed for both signal display and LOD measurements. The LODs were obtained by 200-shot averaging of the REMPI or LIF signal at its maximum with three times the standard deviation of the background noise, which was determined from twenty measurements under the same experimental conditions with no sample in the glass cup.

Our colleagues at the U.S. Army Research Laboratory provided us with the PETN, TNT, and RDX samples. The PETN and TNT samples were obtained from Ensign and Bickford, and Eastman Chemical Company, respectively, whereas the RDX sample (>99% pure) was obtained from recrystallizing an RDX composite gun propellant (M43) twice with an American Chemical Society-specified reagent acetone. Our colleagues at the U.S. Army Corps of Engineers, Waterway Experiment Station, provided us with the soil samples contaminated with known concentrations of RDX. Analysis for energetic material content in these soils was performed according to U.S. Environmental Agency (SW-846) method 8330. We prepared sand samples containing PETN and RDX in the laboratory, and then analyzed them by high-pressure liquid chromatography (ISCCO, Model 2350, Spectra Physics, Model Focus-SM5000).

Concentrations of the energetic materials as a function of temperatures were determined from the global vapor-pressure expressions reported by Dionne et al. [13]. These expressions were derived from both a least-squares fit of their vapor-pressure data, and of data reported by previous workers, which they critically reviewed. The Clausius-Clapeyron expressions for PETN, RDX, and TNT in the temperature range of 278–417 K are as follows:

$$\text{Log P[PETN(ppt)]} = -7243/\text{T(K)} + 25.56, \tag{1}$$

$$\text{Log P[RDX(ppt)]} = -6473/\text{T(K)} + 22.50, \text{ and} \tag{2}$$

$$\text{Log P[TNT(ppb)]} = -5481/\text{T(K)} + 19.37. \quad (3)$$

Stimac [2, 14] reveals, however, that the RDX vapor pressure may be approximately five times greater than that calculated from equation 2.

3. Results and Discussion

3.1 Ultraviolet PF/REMPI. The REMPI excitation spectrum of PETN in the region of 225.8–227 nm is shown in part C of Figure 2. The prominent features are attributed to the $P_{21}+Q_1$, P_1, P_2+Q_{12}, and P_{12} branches of the NO $A^2\Sigma\,\Pi^+ - X^2$ (0,0) band that result from one-photon selection rules ($\Delta J = 0, \pm 1$) that govern the REMPI process. Evident from part C in Figure 2 are the spectral features due to the $^2\Pi_{1/2}$ and $^2\Pi_{3/2}$ spin-orbit components of the NO ground electronic state. The NO spectral features clearly arise through a photofragmentation/fragment ionization mechanism of the PETN vapor that involves the following steps:

$$R-NO_2 \overset{2h\nu_1}{\rightarrow} R + NO\left(X^2\Pi\right) + O \text{ and} \quad (4)$$

$$NO\left(X^2\Pi\right) \overset{h\nu_2}{\rightarrow} NO\left(A^2\Sigma^+\right) \overset{h\nu_2}{\rightarrow} NO^+\left(X^1\Sigma^+\right) + e, \quad (5)$$

where step (4) represents fragmentation of the parent molecule yielding the electronic ground state NO, and step (5) represents the (1+1) REMPI of the NO fragment by means of its $A^2\Sigma^+$ intermediate state. An enhancement of the NO ion signal is observed because the energy of the $A^2\Sigma^+$ state is resonant with the energy of the 227-nm photon. The processes represented by steps (4) and (5) are very fast; they occur within the duration of the laser pulse, ~ 6 ns for our experiment. Also, $h\nu_1 = h\nu_2$ because a single laser operating near 227 nm is used for both fragmentation and fragment ionization. This mechanism is proposed based on our earlier studies of the 227-nm excitation of dimethylnitramine (DMNA), a simple analogue of RDX and PETN, with time-of-flight mass

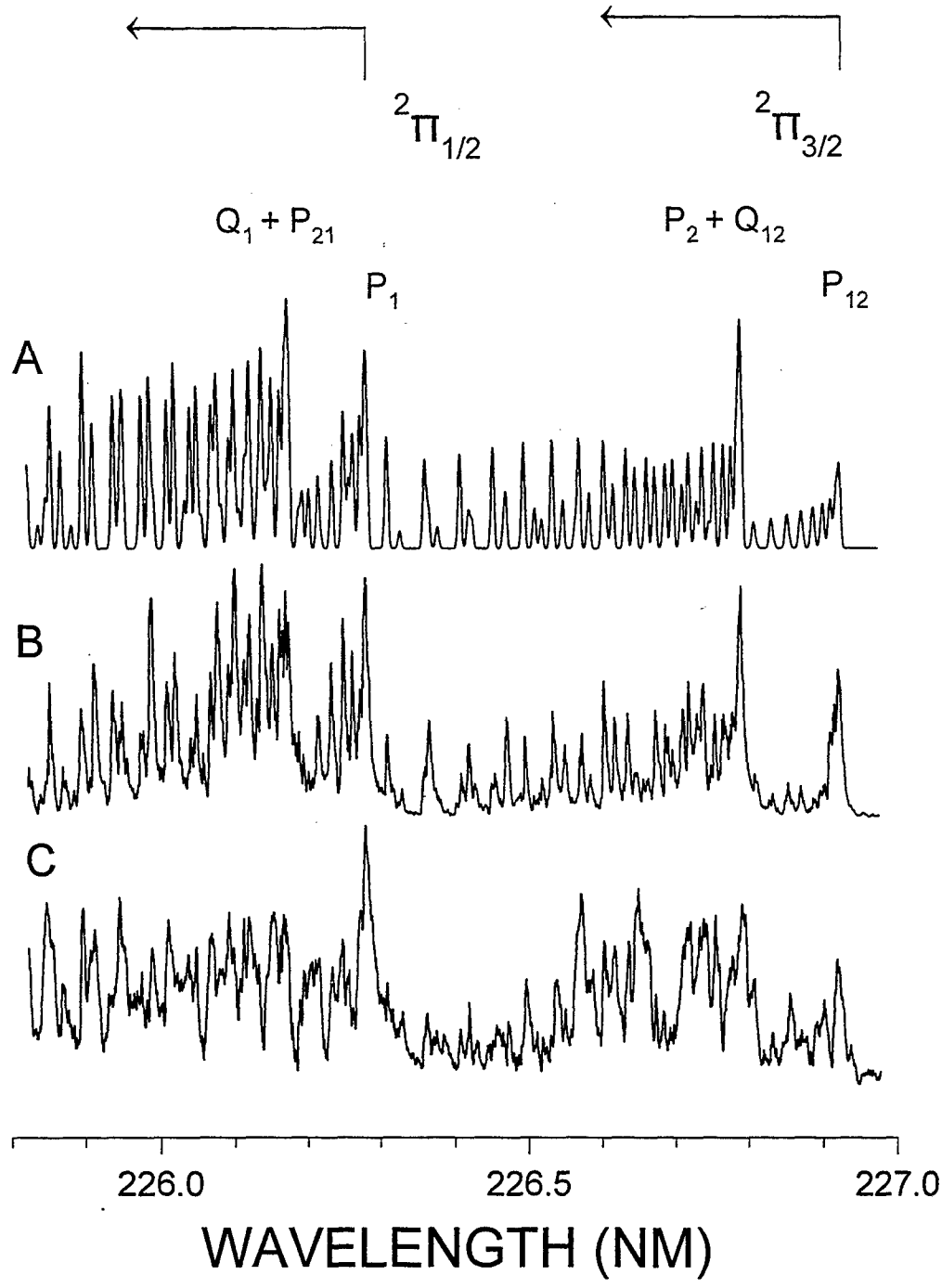

Figure 2. NO Spectra: (a) Computer Simulation, (b) Pyrolysis/LIF of PETN, and (c) PF/REMPI of PETN.

analysis of the fragments [7]. The time-of-flight mass spectrum of DMNA revealed a strong ion signal at a mass-to-charge ratio of 30 that corresponds to the NO^+ ion.

It is important to realize that because the REMPI experiments conducted here are nonselective (i.e., no mass selection is involved), the analytical selectivity of the PF/FD technique depends on laser wavelength excitation for NO detection. As shown in Figure 2 (c), the rotational lines of NO are well-resolved, which confirms that this technique does indeed exhibit sufficient spectral resolution to permit the NO fragment generated from PETN to be identified unequivocally, even at atmospheric pressure and in room air.

The NO^+ signal dependence on the 227-nm laser intensity is measured, and the data are fitted with the equation $S = CI^n$, where S is the ion signal intensity, I is the laser beam intensity, C is a system-dependent constant, and n is the number of photons. The slope of the log-log plot of ion signal vs. intensity yields a value of 1.64 for n. This is somewhat surprising in light of the mechanism already presented which suggests a value of four (i.e., two photons to generate NO from PETN and two photons to produce NO^+). The reason for the lower than expected "n" value is not well understood and is under investigation. The dependence of ion signal on laser intensity suggests that a significant enhancement in sensitivity can be achieved at higher laser intensities. A similar trend is also observed for RDX and TNT.

In Figure 3 (a), a response curve for PETN shows the variation of ion signal with concentration in the 298–393 K temperature range on excitation with 227-nm laser radiation. The PETN sample is heated to different temperatures, and at each temperature the ion signal from the vapor is measured. The concentration at each temperature is calculated using equation 1. We use a similar procedure to obtain the response curves for TNT and RDX in the ranges of 326–393.5 K and 326–416.5 K, respectively.

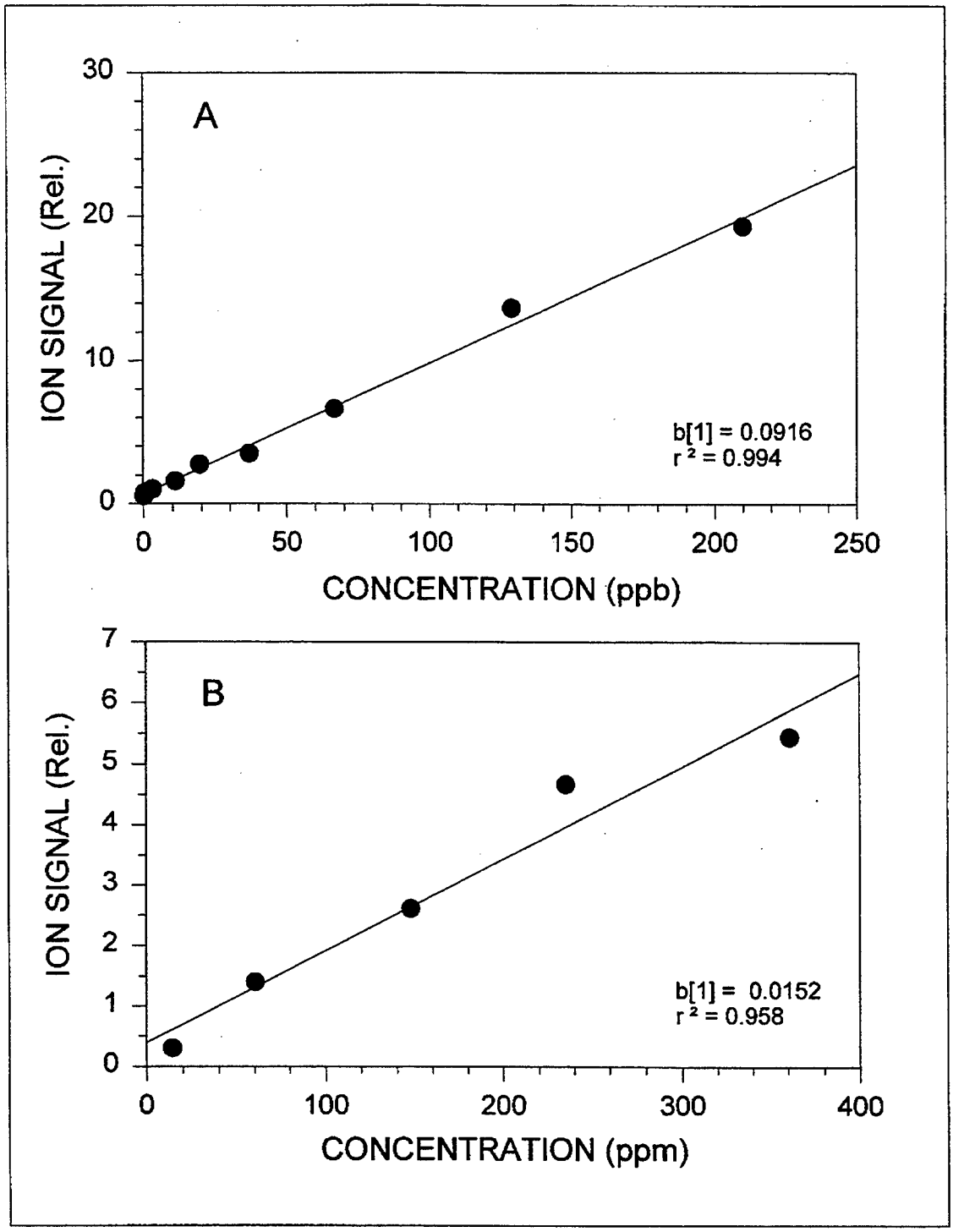

Figure 3. PF/REMPI Response Plots of PETN With (a) ~100 μJ of 227-nm Laser Radiation, and (b) ~5 mJ of 454-nm Laser Radiation.

The LOD in this study is defined as the concentration that produces a signal equal to three times the standard deviation of the background noise divided by the slope of the response curve for a particular compound. Table 1 shows the PF/REMPI LODs for the compounds studied. They are 2 ppb for PETN, 7 ppb for RDX, and 70 ppb for TNT. We calculate the LODs for RDX and TNT by using the vapor-pressure expressions presented in equations 2 and 3, respectively. The high detection sensitivity achieved for PETN indicates that both the photofragmentation and subsequent ionization processes are highly efficient. The lower sensitivity of TNT suggests that its absorption cross-section at 227 nm, the efficacy of NO production, or both, are compared less to PETN and RDX because the photoionization process for NO is the same for all three compounds. It should be noted that the LODs are determined at ambient pressure in room air, suggesting that collisional quenching of the NO ($A^2\Sigma^+$) by N_2 or O_2, and reactions of NO ($A^2\Sigma^+$) with O_2, do not significantly decrease the REMPI signal. The fact that these energetic materials can be detected by PF/REMPI with high sensitivity in room air at ambient pressure without the samples being heated to high temperatures enhances the analytical utility of this technique for field applications.

Table 1. Limits of Detection of PETN, RDX, and TNT

Compound	Wavelength (227 nm)	
	PF/REMPI	PF/LIF
PETN	2 ppb	ND[a]
RDX	7 ppb	ND
TNT	70 ppb	37 ppm

[a]ND = Not determined because the signal is weak, of the order of the background noise.

3.2 Ultraviolet PF/LIF and Pyrolysis/LIF. LIF experiments were also conducted on the same three energetic materials so we could understand their photofragmentation pathways and determine and compare the LOD values with those obtained from REMPI experiments. We determined the PF/LIF LOD of TNT by measuring the LIF signal as a function of its concentration in the 354–397 K temperature range and calculating the LOD by using the same procedures followed for the PF/REMPI experiments. The temperatures used were below 423 K to comply with the vapor-pressure expression presented in equation 3, and to ensure that TNT did not decompose.

Eiceman et al. [14], using a diffusion generator with gravimetry and ion mobility spectrometry, determined that TNT does not decompose at 423 K. The PF/LIF LOD value obtained for TNT is 37 ppm and is listed in Table 1. This value is ~ 500 times greater than that obtained by PF/REMPI. This difference, and the reduced PF/LIF sensitivity for PETN and RDX at lower temperatures, are attributed both to fundamental limitations of the PF/LIF technique and to our system design. Collisional quenching of NO ($A^2\Sigma^+$) by N_2 and O_2, and reactions with O_2 are more pronounced in the LIF experiments than in the REMPI experiments because the radiative lifetime of the $A^2\Sigma^+$ intermediate state is relatively long, ~ 215 ns [15]. In the REMPI experiments, ionization from this state is instantaneous; it occurs within the 6-ns laser pulse and allows little time for quenching and other reactions to occur. A higher sensitivity for REMPI than LIF is also achieved because practically all of the ions produced by REMPI are collected by the electrodes. In contrast, the signal in the LIF experiments is isotropic, and only part of it is collected because it is viewed through a small cone in a direction normal to the excitation laser beam. Collecting more of the signal using parabolic mirrors should yield higher sensitivities.

Wu et al. [10] recently reported their studies of the detection of TNT by PF/LIF. As in our study, a 227-nm laser photofragmented the precursor molecule and subsequently induced fluorescence from the resulting NO fragment. Concentrations of TNT were measured at various temperatures in a low-pressure, static environment. Their research reveals that when the TNT sample was heated from room temperature to 373 K, the LIF intensity did not increase much until the sample temperature reached about 343 K, close to its melting point. At temperatures above 343 K, the LIF intensity increased rapidly with increasing temperature. These results are consistent with our observations on how sample temperature effects the LIF intensity of TNT. The detection limit of TNT was estimated at ~ 0.8 ppm, which was much lower than our LIF results. Possible reasons for the higher sensitivity reported in Wu et al. [10] include the following: (1) the use of higher laser energies, although they are not reported, (2) less collisional quenching of NO ($A^2\Sigma^+$) by N_2 or O_2 and reactions with O_2 in their low-pressure environment, and (3) possible product accumulation of NO, contributing to an increase in the NO LIF signal because of the static environment used in their study.

There is one important difference between the REMPI and LIF experiments of PETN and RDX. Unlike the REMPI experiments, which show a measurable ion signal of NO from PETN even at room temperature, the LIF experiment shows a very weak emission signal below the melting point of PETN, ~413 K. The emission intensity increases sharply above the melting point, and at temperatures above 438 K, the PETN liquid boils so vigorously that rapid sample loss occurs because of evaporation. Light brown vapors from PETN at temperatures above the melting point can be clearly seen, indicating thermal decomposition, possibly to form NO_2. The extent of decomposition at each temperature is not known, however. A similar trend is observed for RDX. The decomposition of RDX is indicated by the distinct but slow color change from white to brown to dark brown at temperatures close to its melting point, 476–477 K; this is followed by vigorous boiling of the liquid and rapid sample loss because of evaporation. TNT, on the other hand, melts at ~353 K, but the light yellow liquid starts to turn brown only around 473 K. The color change becomes more intense and rapid at higher temperatures. Also, unlike RDX and PETN, TNT liquid boils less vigorously and remains in the sample tube for a long time.

In view of the above observations, we used a different approach from PF/REMPI to determine the LODs for PETN and RDX. This approach involved pyrolysis of the energetic material with subsequent detection of the characteristic NO and NO_2 products by LIF and PF/LIF, respectively, near 227 nm. Sand samples contaminated with known amounts of PETN (20.0 ppm) and RDX (24.7 ppm) were placed in a miniature glass cup and then dropped into an oven maintained at predetermined temperatures of 416.5 K for PETN and 471.5 K for RDX. Figure 2 (b) shows the LIF excitation spectrum of PETN in the 225.8–227-nm region, obtained by heating PETN to 413 K. A simulation of the spectrum, shown in Figure 2 (a), is also included for comparison. The simulation was performed using a multiparameter computer program based on a Boltzmann rotational distribution analysis [16, 17]. The program utilizes one-photon line strengths and rotational energy levels calculated using ground and excited electronic spectroscopic constants for NO, which were reported by Henry et al. [18] and Engleman and Rouse [19], respectively and a radiative lifetime was reported by McDermid and Laudenslager [15].

A comparison of Figures 2 (b) and 2 (a) reveals that the observed spectral features from PETN in the region near the electronic origin are identical to those calculated for NO; this suggests that there exists an efficient pathway of PETN that leads to the formation of NO. Figures 2 (a) and 2 (b) also suggest that there is no spectral interference from other fragments that may be produced from PETN because all of the observed spectral features are attributed to NO. This supposition is confirmed by the virtually identical emission spectra for PETN and NO shown in Figure 4. The spectra clearly show a progression in the N-O stretch mode with a frequency of ~1900 cm^{-1} for both NO and NO produced from PETN. Excitation and emission spectral features identical to those of NO were also recorded for RDX and TNT.

Figure 5 shows a signal vs. time curve that we recorded by measuring the LIF signal intensity resulting from 227-nm excitation of PETN as a function of 25-s intervals after the sand sample was dropped into the oven. The LIF intensity rose from zero, went through a maximum, and finally fell to zero as the energetic material, which was initially at room temperature, first melted and then evaporated or decomposed from the sand. The total area under the curve, which we determined using a linear combination of Gaussian and Lorentian functions, represents the amount of PETN evaporated, decomposed, or both, and is assumed to be equal to the initial quantity of PETN. This assumption was verified from high-pressure liquid chromatography analysis of both neat and PETN-doped sand samples before and after the pyrolysis/LIF experiments, which showed that >95% of the PETN decomposed, evaporated, or both. The amount of PETN lost from the mixture during the 25-s interval near the emission maximum was calculated from the ratio of the area under the 25-s segment of the curve at the maximum height to the total area of the curve. The results of a number of these experiments with different amounts of sand yielded the response curves for PETN and RDX that are presented in Figure 6. The LODs were calculated from the slope of the respective response curve using the same procedure previously described, and their values are 2.2 ppm (ng/mg) for PETN and 1.6 ppm (ng/mg) for RDX.

The 227-nm LODs for PETN and RDX, determined by pyrolysis/LIF, are ~3 orders of magnitude greater than those obtained by PF/REMPI. This difference resulted from the fact that the two methods are mechanistically different. The REMPI measurements involve laser

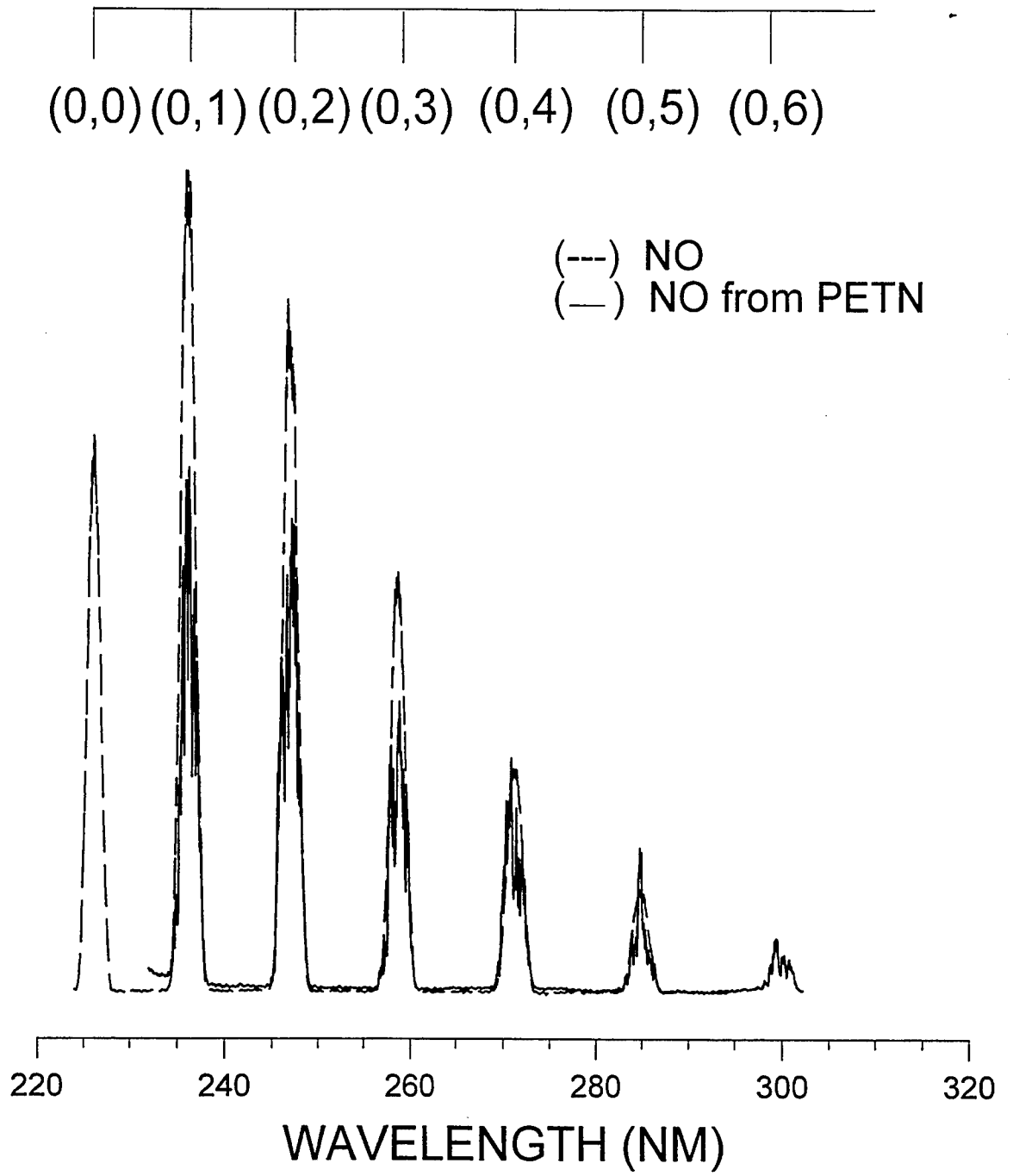

Figure 4. 227-nm LIF Emission Spectra of 0.1% NO in N_2 at Room Temperature and NO From PETN.

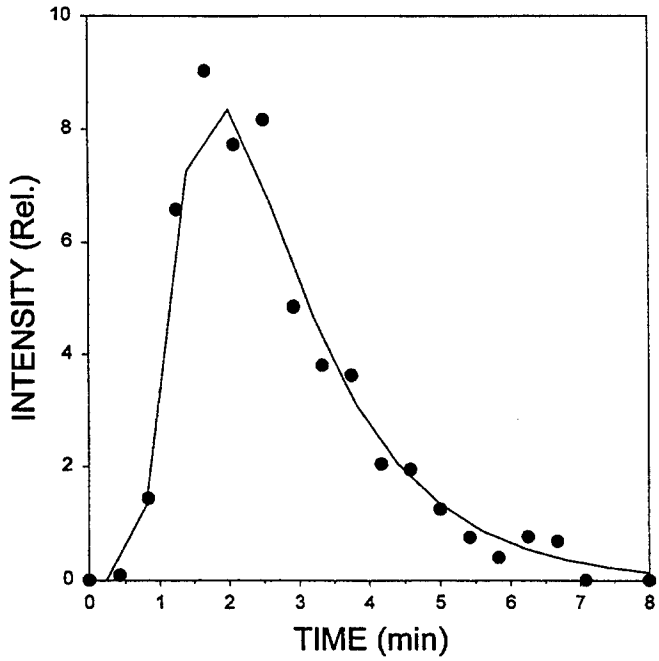

Figure 5. Intensity vs. Time Plot of NO From 20 ppm of PETN in Sand.

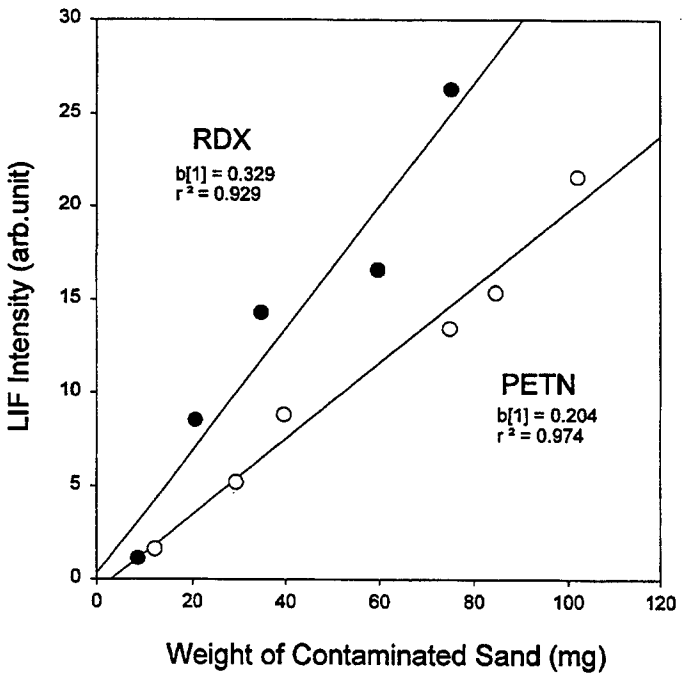

Figure 6. Pyrolysis/LIF Response Curves of NO From RDX (•) and PETN (○).

photofragmentation of the precursor molecule to NO with subsequent NO ionization. In contrast, the LIF measurements involve pyrolysis of the precursor molecule to NO with subsequent NO LIF at 227 nm, or pyrolysis of the precursor molecule to NO_2 with subsequent NO_2 laser photofragmentation to NO, followed by laser excitation of NO. This mechanism is consistent with open literature reports on pyrolysis of RDX [20–23] and PETN [14, 24, 25].

3.3 Visible PF/REMPI and Pyrolysis/LIF. PF/FD experiments on the energetic materials were also performed with a visible laser because of the potential advantages offered by a visible laser over an ultraviolet laser. A PF/REMPI response curve for PETN at 453.85 nm is presented in Figure 3 (b). The slope of the response curve, together with the noise, yields a LOD of 16 ppm. This value is several orders of magnitude higher than that obtained at 227 nm and is attributed to (1) the lower photofragmentation efficiency of the precursor molecule to generate NO, and (2) the lower NO ionization efficiency when visible laser radiation rather than ultraviolet laser radiation is used. Although the PF/REMPI technique at 454 nm is less sensitive than that at 227 nm, it is still very useful for many applications, including those involving the analysis of underground contaminated soil with laser-based, cone-penetrometer systems. The PF/REMPI technique would be useful for such applications because of the modest sensitivities needed, typically hundreds of ppm, and because the laser beam can easily be transmitted distances over 10–30 m through optical fibers.

Figure 7 shows the LIF excitation spectra of NO and NO generated from the pyrolysis of PETN in the 452–454 nm region. The spectral features of NO from PETN are identical to those that result from the two-photon excitation of NO by means of its $A^2\Sigma^+ - X^2\Pi$ (0,0) band. The emission spectrum recorded following 454-nm laser excitation is also identical to the emission spectrum of NO shown in Figure 4. These observations reconfirm the fact that NO is a major stable product of the decomposition of PETN. The LOD for PETN is 140 ppm (ng/mg), approximately nine times greater than that produced by PF/REMPI at the same wavelength. The LODs for RDX and TNT are not reported because the NO LIF signals were of the order of the background noise.

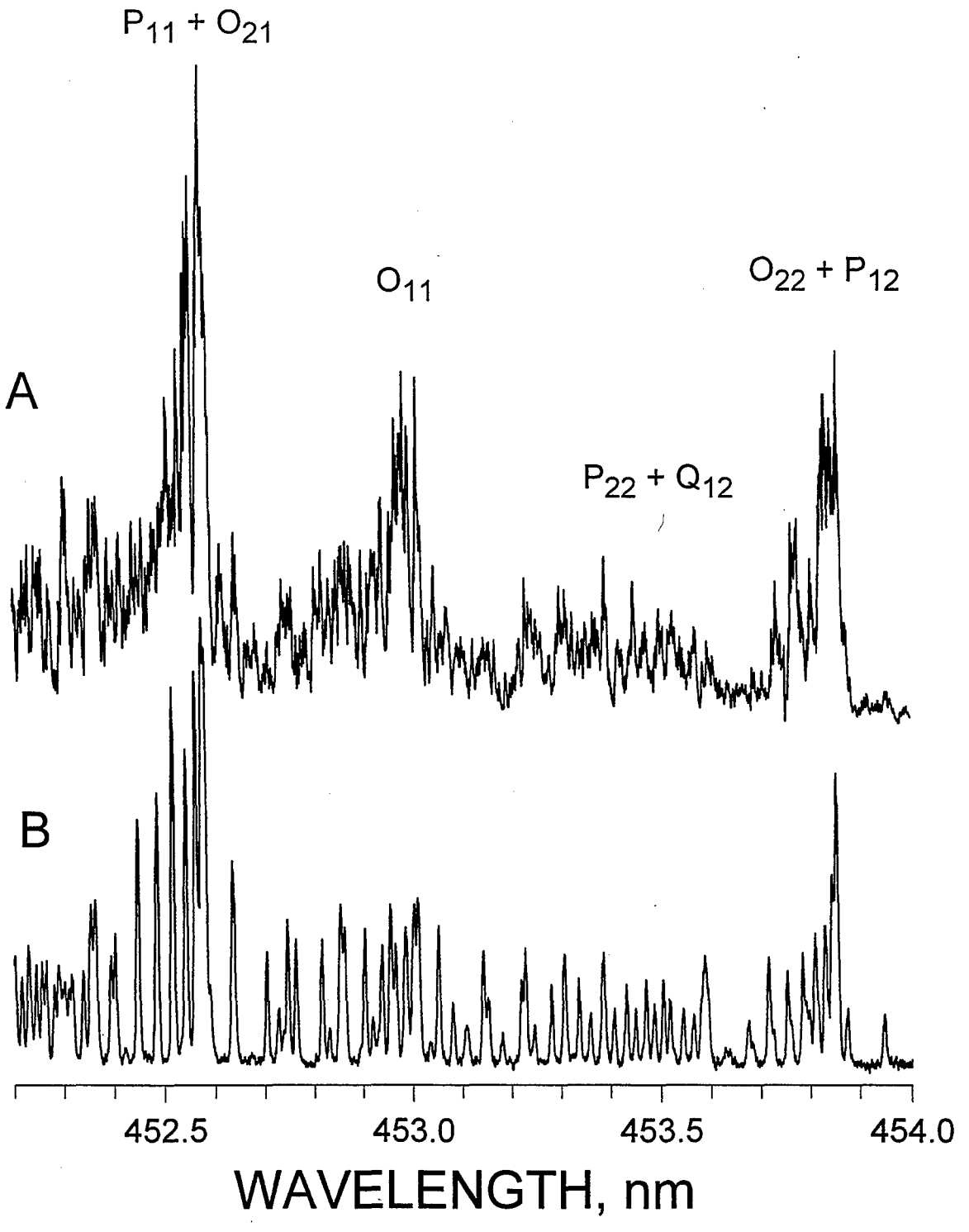

Figure 7. Two-Photon LIF Excitation Spectrum of NO From (a) PETN and (b) 0.1% NO in N_2.

4. Conclusion

The analytical utility of PF/FD spectroscopy and pyrolysis/LIF spectroscopy has been demonstrated for the trace detection of PETN, RDX, and TNT in air (at atmospheric pressure) using both ultraviolet and visible laser radiation. In the PF/FD technique, a laser operating at 227 or 454 nm photofragments the energetic material and facilitates detection of the characteristic NO fragment by REMPI or LIF, using the NO $A^2\Sigma^+ - X^2\Pi$ (0,0) transitions near 227 nm. In contrast, the pyrolysis/LIF technique involves pyrolysis of the energetic material with subsequent detection of the NO and NO_2 products by LIF and PF/LIF, respectively. The PF/REMPI, PF/LIF, and pyrolysis/LIF excitation spectra unequivocally reveal the presence of NO without any spectral interference from other photolysis products and that the NO rotational lines are well-resolved at atmospheric pressure. This result indicates that these techniques can be highly selective on the basis of wavelength. The LIF emission spectra also reveal several NO spectral features in the 220–305-nm range, which can be used as an additional fingerprint for NO detection, thus enhancing the selectivity of the method.

We could measure all three energetic compounds by 227-nm PF/REMPI without heating the sample. The LODs ranged from 2 to 70 ppb, with PETN having the highest sensitivity. The differences in the sensitivities are attributed to the differences in NO generation because the NO detection efficiency is the same for all three compounds. The PF/REMPI LOD of PETN at 454 nm is 16 ppm. This value is much greater than that obtained using 227-nm radiation and is attributed to the lower NO formation and higher ionization efficiencies in the visible laser radiation than in the ultraviolet laser radiation. The PF/LIF LOD value of TNT at 227 nm is 37 ppm. This value is greater than that obtained by PF/REMPI at the same wavelength and is attributed to a lower NO detection efficiency. The pyrolysis/LIF LODs of PETN ranged from low ppm for PETN and RDX at 227 nm, to 140 ppm for PETN at 454 nm. The lower sensitivity at 454 nm than at 227 nm results from a lower NO excitation efficiency in the visible than in the ultraviolet.

The PF/REMPI approach exhibits great potential for detecting trace levels of energetic materials in real-time and *in situ* because of its high sensitivity, selectivity, and instrumentation simplicity. An

increase in sensitivity is projected for both PF/FD and pyrolysis/LIF techniques with the use of higher pulse energies and for LIF-based techniques by improving the system design.

Note Added in Proof. We have recently performed PF/LIF experiments on neat RDX and TNT at 1 atm and in room air with 227-nm radiation and a photomultiplier tube/interference filter configuration; we determined their LODs to be in the low ppm.

INTENTIONALLY LEFT BLANK.

5. References

1. Simeonsson, J. B., and R. C. Sausa. "Laser Photofragmentation/Fragment Detection Techniques for Chemical Analysis of the Gas-Phase." *Trends Analytical Chemistry*, vol. 17, nos. 8 and 9, pp. 542–550, 1998.

2. Steinfeld, J. I., and J. Wormhoudt. "Explosives Detection: A Challenge for Physical Chemistry." *Annual Review of Physical Chemistry*, vol. 49, pp. 203–232, 1998.

3. Simeonsson, J. B., and R. C. Sausa. "A Critical Review of Laser Photofragmentation/ Fragment Detection Techniques for Gas Phase Chemical Analysis." *Applied Spectroscopy Reviews*, vol. 31, pp. 1–72, 1996.

4. Huang, S. D., L. Kolaitis, and D. M. Lubman. "Detection Of Explosives Using Laser Desorption/Mass Spectrometry." *Applied Spectroscopy*, vol. 41, pp. 1371–1376, 1987.

5. Riris, H., C. B. Carisle, D. F. McMillen, and D. E. Cooper. "Explosives Detection With a Frequency Modulation Spectrometer." *Applied Optics*, vol. 35, pp. 4694–4704, 1996.

6. Capellos, C., P. Papagiannakopoulos, and Y. Liang. "The 248-nm Photodecomposition of Hexahydro-1,3,5-Trinitro-1,3,5-Triazine." *Chemical Physics Letters*, vol. 164, no. 5, pp. 533–538, 1989.

7. Lemire, G. W., J. B. Simeonsson, and R. C. Sausa. "Monitoring of Vapor-Phase Nitrocompounds Using 226-nm Radiation: Fragmentation With Subsequent NO Resonance-Enhanced Multiphoton Ionization Detection." *Analytical Chemistry*, vol. 65, pp. 529–533, 1994.

8. Clark, A., K. W. D. Ledingham, A. Marshall, J. Sander, and R. P. Singhal. "Attomole Detection of Nitroaromatic Vapors Using Resonance-Enhanced Multiphoton Ionization Mass-Spectrometry." *Analyst*, vol. 118, no. 6, pp. 601–607, 1993.

9. Simeonsson, J. B., G. W. Lemire, and R. C. Sausa. "Trace Detection of Nitrocompounds by ArF Laser Photofragmentation/Ionization Spectrometry." *Applied Spectroscopy*, vol. 47, no. 11, pp. 1907–1912, 1993.

10. Wu, D., J. Singh, F. Yueh, and D. Monts. "2,4,6-Trinitrotoluene Detection by Laser-Photofragmentation/Laser-Induced Fluorescence." *Applied Optics*, vol. 35, no. 21, pp. 3998–4003, 1996.

11. Boudreaux, G. M., T. S. Miller, A. J. Kunefke, J. P. Singh, F. Yueh, and D. Monts. "Development of a Photofragmentation Laser-Induced Fluorescence Sensor for Detection of 2,4,6-Trinitrotoluene in Soil and Groundwater." *Applied Optics*, vol. 38, no. 6, pp. 1411–1417, 1999.

12. Davis, W. M., E. R. Cespedes, L. T. Lee, J. F. Powell, and R. A. Goodson. "Rapid Delineation of Subsurface Petrolium Contamination Using the Site Characterization and Analysis Penetrometer System." *Environmental Geology*, vol. 29, pp. 228–237, 1997.

13. Dionne, B. C., D. P. Rounbehler, E. K. Achter, J. R. Hobbs, and D. H. Fine. "Vapor Pressure of Explosives." *Journal of Energetic Materials*, vol. 4, pp. 447–472, 1986.

14. Eiceman, G. A., D. Preston, G. Tiano, J. Rodriguez, and J. E. Parmeter. "Quantitative Calibration of Vapor Levels of TNT, RDX, and PETN Using a Diffusion Generator With Gravimetry and Ion Mobility Spectrometry." *Talanta*, vol. 45, pp. 57–74, 1997.

15. McDermid, I. S., and J. B. Laudenslager. "Radiative Lifetimes and Electronic Quenching Rate Constants for Single-Photon Excited Rotational Levels of NO ($A^2\Sigma^+$, $v' = 0$)." *Journal of Quantitative Spectroscopy and Radiative Transfer*, vol. 27, no. 5, pp. 483–492, 1982.

16. Simeonsson, J. B., and R. C. Sausa. "Trace Analysis of NO_2 in the Presence of NO by Laser Photofragmentation/Fragment Photoionization Spectrometry at Visible Wavelengths." *Applied Spectroscopy*, vol. 50, no. 10, pp. 1277–1282, 1996.

17. Vanderhoff, J. A., M. W. Teague, and A. J. Kotlar. "Detection of Temperature and NO Concentrations Through the Dark Zone of Solid-Propellant Flames." *Proceedings of the 24th Symposium (International) on Combustion*, The Combustion Institute, Pittsburgh, PA, pp. 1915–1922, 1992.

18. Henry, A., M. F. Le Moal, P. Cardinet, and A. Valentin. "Overtone Bands of $^{14}N^{16}O$ and Determination of Molecular Constants." *Journal Molecular Spectroscopy*, vol. 70, no. 1, pp. 18–26, 1978.

19. Engleman, Jr., R., and P. E. Rouse. "The β and γ Bands of Nitric Oxide Observed During Flash Photolysis of Nitrosyl Chloride." *Journal Molecular Spectroscopy*, vol. 37, pp. 240–251, 1971.

20. Ermolin, N. E., and V. E. Zarko. "Mechanism and Kinetics of the Thermal Decomposition of Cyclic Nitramines." *Combustion, Explosion, and Shock Waves*, vol. 33, no. 3, pp. 251–269, 1997.

21. Behrens, R., and S. Bulusu. "Thermal Decomposition of Energetic Materials 3: Temperal Behaviors of the Rates of Formation of the Gaseous Pyrolysis Products From Condensed-Phase Decomposition of 1,3,5-Trinitrohexahydro-s-triazine." *Journal of Physical Chemistry*, vol. 96, no. 22, pp. 8877–8891, 1992.

22. Behrens, R., and S. Bulusu. "Thermal Decomposition of Energetic Materials 4: Deuterium Isotope Effects and Isotopic Scrambling (H/D, $^{13}C/^{18}O$, $^{14}N/^{15}N$) in Condensed-Phase Decomposition of 1,3,5-Trinitrohexahydro-s-triazine." *Journal of Physical Chemistry*, vol. 96, no. 22, pp. 8891–8897, 1992.

23. Oyumi, Y., and T. Brill. "Thermal Decomposition of Energetic Materials 3: A High-Rate in situ, FTIR Study of the Thermolysis of RDX and HMX With Pressure and Heating Rates as Variables." *Combustion and Flame*, vol. 62, pp. 213–224, 1985.

24. Oyumi, Y., and T. Brill. "Thermal Decomposition of Energetic Materials 4: Selective Product Distributions Evidenced in Rapid, Real-Time Thermolysis of Nitrate Esters at Various Pressures." *Combustion and Flame*, vol. 66, no. 9, pp. 9–16, 1986.

25. Ng, W. L., J. E. Field, and H. M. Hauser. "Study of Thermal Decomposition of Pentaerythritol Tetranitrate." *Journal Chemistry Social Perkin Translation*, vol. 2, no. 6, pp. 637–639, 1976.

INTENTIONALLY LEFT BLANK.

NO. OF COPIES	ORGANIZATION
2	DEFENSE TECHNICAL INFORMATION CENTER DTIC DDA 8725 JOHN J KINGMAN RD STE 0944 FT BELVOIR VA 22060-6218
1	HQDA DAMO FDT 400 ARMY PENTAGON WASHINGTON DC 20310-0460
1	OSD OUSD(A&T)/ODDDR&E(R) R J TREW THE PENTAGON WASHINGTON DC 20301-7100
1	DPTY CG FOR RDA US ARMY MATERIEL CMD AMCRDA 5001 EISENHOWER AVE ALEXANDRIA VA 22333-0001
1	INST FOR ADVNCD TCHNLGY THE UNIV OF TEXAS AT AUSTIN PO BOX 202797 AUSTIN TX 78720-2797
1	DARPA B KASPAR 3701 N FAIRFAX DR ARLINGTON VA 22203-1714
1	US MILITARY ACADEMY MATH SCI CTR OF EXCELLENCE MADN MATH MAJ HUBER THAYER HALL WEST POINT NY 10996-1786
1	DIRECTOR US ARMY RESEARCH LAB AMSRL D D R SMITH 2800 POWDER MILL RD ADELPHI MD 20783-1197

NO. OF COPIES	ORGANIZATION
1	DIRECTOR US ARMY RESEARCH LAB AMSRL DD 2800 POWDER MILL RD ADELPHI MD 20783-1197
1	DIRECTOR US ARMY RESEARCH LAB AMSRL CI AI R (RECORDS MGMT) 2800 POWDER MILL RD ADELPHI MD 20783-1145
3	DIRECTOR US ARMY RESEARCH LAB AMSRL CI LL 2800 POWDER MILL RD ADELPHI MD 20783-1145
1	DIRECTOR US ARMY RESEARCH LAB AMSRL CI AP 2800 POWDER MILL RD ADELPHI MD 20783-1197
	ABERDEEN PROVING GROUND
4	DIR USARL AMSRL CI LP (BLDG 305)

NO. OF COPIES	ORGANIZATION
	ABERDEEN PROVING GROUND
20	DIR USARL AMSRL WM BD B E FORCH W R ANDERSON S W BUNTE C F CHABALOWSKI A COHEN R DANIEL D DEVYNCK R A FIFER B E HOMAN A J KOTLAR K L MCNESBY M MCQUAID M S MILLER A W MIZIOLEK J B MORRIS R A PESCE-RODRIGUEZ B M RICE R C SAUSA M A SCHROEDER J A VANDERHOFF

REPORT DOCUMENTATION PAGE

Form Approved
OMB No. 0704-0188

1. AGENCY USE ONLY *(Leave blank)*	2. REPORT DATE	3. REPORT TYPE AND DATES COVERED
	February 2001	Final, Jan 97–Dec 99

4. TITLE AND SUBTITLE
Detection of Energetic Materials by Laser Photofragmentation/Fragment Detection and Pyrolysis/Laser-Induced Fluorescence

5. FUNDING NUMBERS
611102.AH43

6. AUTHOR(S)
Rosario C. Sausa, Vaidhianat Swayambunathan, and Gurbax Singh*

7. PERFORMING ORGANIZATION NAME(S) AND ADDRESS(ES)
U.S. Army Research Laboratory
ATTN: AMSRL-WM-BD
Aberdeen Proving Ground, MD 21005-5066

8. PERFORMING ORGANIZATION REPORT NUMBER
ARL-TR-2387

9. SPONSORING/MONITORING AGENCY NAMES(S) AND ADDRESS(ES)

10.SPONSORING/MONITORING AGENCY REPORT NUMBER

11. SUPPLEMENTARY NOTES
* University of Maryland Eastern Shore, Department of Natural Sciences

12a. DISTRIBUTION/AVAILABILITY STATEMENT
Approved for public release; distribution is unlimited.

12b. DISTRIBUTION CODE

13. ABSTRACT*(Maximum 200 words)*

Trace concentrations of energetic materials such as 2,4,6-trinitrotoluene (TNT), pentaerythritol tetranitrate (PETN), and hexahydro-1,3,5-trinitro-s-triazine (RDX) are detected by laser photofragmentation/fragment detection (PF/FD) spectrometry. In this technique, a single laser operating near 227 nm photofragments the parent molecule and facilitates the detection of the characteristic NO fragment by means of its $A^2\Sigma^+ - X^2\ \Pi$ (0,0) transitions near 227 nm. Fragment detection is accomplished by resonance-enhanced multiphoton ionization (REMPI) with miniature electrodes and by laser-induced fluorescence (LIF) with a photodetector. Experiments are also conducted in the visible region using 453.85-nm radiation for photofragmentation and fragment detection. Sand samples contaminated with PETN and RDX are analyzed by a pyrolysis/LIF technique, which involves pyrolysis of the energetic material with subsequent detection of the pyrolysis products NO and NO_2 by LIF and PF/LIF, respectively, near 227 nm. Applying these techniques to the trace analysis of TNT, PETN, and RDX at ambient pressure in room air is demonstrated with limits of detection (S/N = 3) in the range of low parts-per-billion to parts-per-million for a 20-s integration time with 10–120 μJ of laser energy at 226.8 nm and ~ 5 mJ at 453.85 nm. An increase in detection sensitivity is projected with an increase in laser energy and an improved system design. The analytical merits of these techniques are discussed and compared to other laser-based techniques.

14. SUBJECT TERMS	15. NUMBER OF PAGES
laser photofragmentation/fragment detection, pyrolysis/laser-induced fluorescence, energetic material detection, TNT, PETN	30
	16. PRICE CODE

17. SECURITY CLASSIFICATION OF REPORT	18. SECURITY CLASSIFICATION OF THIS PAGE	19. SECURITY CLASSIFICATION OF ABSTRACT	20. LIMITATION OF ABSTRACT
UNCLASSIFIED	UNCLASSIFIED	UNCLASSIFIED	UL

INTENTIONALLY LEFT BLANK.

USER EVALUATION SHEET/CHANGE OF ADDRESS

This Laboratory undertakes a continuing effort to improve the quality of the reports it publishes. Your comments/answers to the items/questions below will aid us in our efforts.

1. ARL Report Number/Author ARL-TR-2387 (Sausa) Date of Report February 2001

2. Date Report Received _____

3. Does this report satisfy a need? (Comment on purpose, related project, or other area of interest for which the report will be used.) _____

4. Specifically, how is the report being used? (Information source, design data, procedure, source of ideas, etc.) _____

5. Has the information in this report led to any quantitative savings as far as man-hours or dollars saved, operating costs avoided, or efficiencies achieved, etc? If so, please elaborate. _____

6. General Comments. What do you think should be changed to improve future reports? (Indicate changes to organization, technical content, format, etc.) _____

CURRENT ADDRESS

_____
Organization

_____
Name E-mail Name

_____
Street or P.O. Box No.

_____
City, State, Zip Code

7. If indicating a Change of Address or Address Correction, please provide the Current or Correct address above and the Old or Incorrect address below.

OLD ADDRESS

_____
Organization

_____
Name

_____
Street or P.O. Box No.

_____
City, State, Zip Code

(Remove this sheet, fold as indicated, tape closed, and mail.)

(DO NOT STAPLE)